

This discussion paper is/has been under review for the journal Geoscientific Model Development (GMD). Please refer to the corresponding final paper in GMD if available.

Simulating the mid-Pliocene Warm Period with the CCSM4 model

N. A. Rosenbloom, B. L. Otto-Bliesner, E. C. Brady, and P. J. Lawrence

National Center for Atmospheric Research, 1850 Table Mesa Drive, Boulder, CO 80305, USA

Received: 27 November 2012 – Accepted: 4 December 2012 – Published: 13 December 2012

Correspondence to: N. A. Rosenbloom (nanr@ucar.edu)

Published by Copernicus Publications on behalf of the European Geosciences Union.

GMDD

5, 4269–4303, 2012

Simulating the mid-Pliocene Warm Period with the CCSM4 model

N. A. Rosenbloom et al.

[Title Page](#)

[Abstract](#)

[Introduction](#)

[Conclusions](#)

[References](#)

[Tables](#)

[Figures](#)



[Back](#)

[Close](#)

[Full Screen / Esc](#)

[Printer-friendly Version](#)

[Interactive Discussion](#)

Abstract

This paper describes the experimental design and model results from a 500 yr fully coupled Community Climate System Model (v4) simulation of the mid-Pliocene Warm Period (mPWP) (ca. 3.3 to 3.0 Ma). We simulate the mPWP using the “alternate” protocol prescribed by the Pliocene Model Intercomparison Project (PlioMIP) for the AOGCM simulation (Experiment 2). Results from the CCSM4 mPWP simulation show a 1.9°C increase in global mean annual temperature compared to the 1850 preindustrial control, with a polar amplification of ~3 times the global warming. Global precipitation increases slightly by 0.09 mm day⁻¹ and the monsoon rainfall is enhanced, particularly in the Northern Hemisphere. Areal sea ice extent decreases in both hemispheres but persists through the summers. The model simulates a relaxation of the zonal SST gradient in the tropical Pacific, with the El Niño-Southern Oscillation (Niño3.4) ~20% weaker than the preindustrial and exhibiting extended periods of quiescence of up to 150 yr. The maximum Atlantic Meridional Overturning Circulation and northward Atlantic oceanic heat transport are indistinguishable from the control. As compared to PRISM3, CCSM4 overestimates Southern Hemisphere (SH) sea surface temperatures, but underestimates Northern Hemisphere (NH) warming, particularly in the North Atlantic suggesting that an increase in northward ocean heat transport would bring CCSM4 SSTs into better alignment with proxy data.

1 Introduction

We present results from a 500 yr model simulation of the mid-Pliocene Warm Period (mPWP) using the Community Climate System Model, version 4 (CCSM4). The mid-Pliocene Warm Period (ca. 3.3 to 3.0 Ma) is the last period of sustained warmth before the onset of Pleistocene glaciation. Temperature reconstructions from proxies point to a 2 to 3°C increase in mean global surface temperature over present day (Dowsett, 2007), with high latitude temperatures as much as 15 to 20°C warmer than

GMDD

5, 4269–4303, 2012

Simulating the mid-Pliocene Warm Period with the CCSM4 model

N. A. Rosenbloom et al.

[Title Page](#)

[Abstract](#)

[Introduction](#)

[Conclusions](#)

[References](#)

[Tables](#)

[Figures](#)



[Back](#)

[Close](#)

[Full Screen / Esc](#)

[Printer-friendly Version](#)

[Interactive Discussion](#)



Simulating the mid-Pliocene Warm Period with the CCSM4 model

N. A. Rosenbloom et al.

[Title Page](#)

[Abstract](#)

[Introduction](#)

[Conclusions](#)

[References](#)

[Tables](#)

[Figures](#)



[Back](#)

[Close](#)

[Full Screen / Esc](#)

[Printer-friendly Version](#)

[Interactive Discussion](#)



modern (Ballantyne et al., 2010). The mPWP is also the last prolonged period in Earth history when CO₂ concentrations were similar to present day. It is, therefore, of particular interest because unlike other warm periods in Earth history, we have relatively abundant proxy data that provide good estimates of both land and ocean temperatures.

5 However, the enigma of the mPWP is that although continental configurations and ocean bathymetry were close to modern and estimated CO₂ concentrations (405 ppmv; Pagani, 2010) were only incrementally higher than current day values (391 ppm (October 2012, Mauna Loa (<http://www.esrl.noaa.gov/gmd/ccgg/trends/>)), proxy evidence reveals a much lower pole-to-equator temperature gradient and a more equable seasonal climate overall (Ballantyne et al., 2010). By simulating the mid-Pliocene and comparing it to proxy records which show evidence of a strong climate response to CO₂ forcing, we look through an imperfect lens onto a warm world in hopes that it may help us understand the response of future climate to increasingly higher concentrations of atmospheric greenhouse gases. In the process we test the ability of the CCSM4 model to sustain an alternate state of the Earth climate system that looks very different from that of the present day.

2 Model description

To simulate the mid-Pliocene we use CCSM4 (Gent et al., 2011), which has active atmosphere, land, ocean, and sea ice component models that are linked through a coupler that exchanges state information and fluxes between the components.

2.1 Atmosphere

The atmosphere component model in CCSM4 is the Community Atmosphere Model (CAM4) (Neale et al., 2012). The CAM4 model changed from the spectral core used in CCSM3/CAM3, to the Lin-Rood finite volume core (Lin, 2004). The CAM4 model has improved spatial and temporal aspects of ENSO over the CAM3 model (Richter

and Rasch, 2008; Neale et al., 2008; Deser et al., 2011). Changes to cloud fraction calculations improve Arctic cloud formation and lead to a more realistic polar response. However comparisons with satellite observations indicate that CAM4 continues to have long-standing cloud biases (Kay et al., 2012a), which tend to suppress surface warming and sea ice loss in the Arctic (Kay et al., 2012b). We use a $\sim 1^\circ$ horizontal grid for CAM4, with 192×288 latitude/longitude grid cells and a uniform resolution of 0.9° in latitude $\times 1.25^\circ$ in longitude. CAM4 uses 26 layers in the vertical, which are distributed similarly to CAM3.

2.2 Land

The CCSM4 uses the Community Land Model, version 4 (Lawrence et al., 2012). The CLM4 model differs from CLM3, used in CCSM3, by the addition of a carbon-nitrogen (CN) biogeochemical model, revised hydrology, landcover and land use algorithms, and soil and snow submodels. These modifications lead to improvements in soil water storage, evapotranspiration, surface albedo, and permafrost in fully coupled CCSM4 simulations. The global land precipitation bias is larger in CCSM4 relative to CCSM3, but the global land air temperature bias is reduced and the annual cycle is improved, especially in high latitudes. CCSM4/CLM4 relies on an embedded River Transport Model (RTM, Branstetter and Famiglietti, 1999) to carry gridcell runoff to the ocean along a model approximation of real world river networks. The land (CLM4) and atmosphere (CAM4) component models share the same 0.9° latitude $\times 1.25^\circ$ longitude horizontal grid; RTM resolution is 0.5° latitude/longitude grid.

2.3 Ocean

The CCSM4 ocean component model (POP2) is based on the “Parallel Ocean Program”, version 2 (Smith et al., 2010). We use the standard CCSM4 displaced pole ocean grid with poles in Greenland and Antarctica. The ocean grid has 320×384 points with nominally 1° resolution except near the equator where the latitudinal resolution

Simulating the mid-Pliocene Warm Period with the CCSM4 model

N. A. Rosenbloom et al.

[Title Page](#)

[Abstract](#)

[Introduction](#)

[Conclusions](#)

[References](#)

[Tables](#)

[Figures](#)

[⏪](#)

[⏩](#)

[◀](#)

[▶](#)

[Back](#)

[Close](#)

[Full Screen / Esc](#)

[Printer-friendly Version](#)

[Interactive Discussion](#)



Simulating the mid-Pliocene Warm Period with the CCSM4 model

N. A. Rosenbloom et al.

[Title Page](#)

[Abstract](#)

[Introduction](#)

[Conclusions](#)

[References](#)

[Tables](#)

[Figures](#)

⏪

⏩

◀

▶

[Back](#)

[Close](#)

[Full Screen / Esc](#)

[Printer-friendly Version](#)

[Interactive Discussion](#)



becomes finer as described in Danabasoglu et al. (2006). The number of vertical levels in the ocean increased from 40 to 60 in CCSM4, allowing for twenty 10 m levels in the upper ocean. A new overflow parameterization was added to represent density driven flows in the Denmark Strait, Faroe Bank Channel, Ross Sea and Weddell Sea (Danabasoglu et al., 2010; Briegleb et al., 2010). Overall, the CCSM4 ocean model shows clear improvement in reducing sea surface temperature (SST) and sea surface salinity (SSS) biases relative to the CCSM3 (Gent et al., 2011; Danabasoglu et al., 2012), notably in the North Atlantic where slight changes in the Gulf Stream and North Atlantic Currents reduce but do not eliminate the negative SST and fresh SSS biases along the North Atlantic Current path, while increasing the warm SST and saline biases off the North American Coast. Despite these improvements, the ocean model continues to lose significant heat content for the duration of the preindustrial control simulation (Danabasoglu et al., 2012). Maximum North Atlantic overturning (> 24 Sv) is stronger in CCSM4 than it was in CCSM3 (> 20 Sv) (Gent et al., 2011). Changes to horizontal viscosities along coastal cells (Jochum et al., 2008) support deep water formation in the southern Labrador Sea in CCSM4, instead of farther east in the North Atlantic where it incorrectly occurred in CCSM3.

2.4 Sea ice

The CCSM4 sea ice component model (CICE4) is based on version 4 of the Los Alamos National Laboratory “Community Ice Code” sea ice model (Hunke and Lipscomb, 2008). The sea ice component models in CCSM3 and CCSM4 are generally similar. However, CICE4 incorporates a sophisticated new shortwave radiative transfer scheme that significantly improves the representation of sea ice radiative transfer by using inherent optical properties to define scattering and absorption characteristics of snow and ice. The new model also explicitly accounts for melt ponds and the radiative impacts of aerosols on sea ice. The radiative impact of melt ponds and aerosols on preindustrial Arctic sea ice is 1.1 W m^{-2} annually (Holland et al., 2012), whereas they have negligible impact on Antarctic sea ice. In general, Arctic sea ice thickness,

areal extent and spatial pattern compare well to observations in the CCSM4 twentieth-century simulations (Jahn et al., 2012). CCSM4 sea ice extents in the Labrador Sea and adjacent North Atlantic have been reduced relative to CCSM3, and the southern Labrador Sea is now ice free. Antarctic sea ice distribution is similar to CCSM3, but still too extensive relative to observations. CICE4 uses the same horizontal grid as the ocean component (POP2).

3 Experimental design of Pliocene simulation

This simulation is one of a coordinated set of model experiments, collectively known as the Pliocene Model Intercomparison Project (PlioMIP). PlioMIP is part of the broader scale Paleoclimate Modeling Intercomparison Project (PMIP3; <http://pmip3.lscce.ipsl.fr/>). The first phase of PlioMIP includes two modeling experiments (Haywood et al., 2010, 2011). The first experiment compares atmosphere-only (AGCM) climate models; the second contrasts fully coupled ocean-atmosphere (AOGCM) climate models. In this paper we outline the implementation we used to complete the second, fully coupled experiment (Haywood et al., 2011) with the CCSM4 climate model. NCAR did not undertake the atmosphere-only (AGCM) experiment.

The PlioMIP models use forcing and boundary conditions specified by the USGS Pliocene Research Interpretation and Synoptic Mapping project, version 3 (PRISM3; <http://geology.er.usgs.gov/eespteam/prism/>). The PlioMIP protocol for the AOGCM experiment outlines two model configurations: “preferred” and “alternate”, and PRISM3 provides separate boundary condition data packages to accommodate each configuration. The “preferred” data package includes a land/sea mask that is faithful to what is known about the mPWP, including removal of the West Antarctic Ice Sheet (WAIS). The “alternate” configuration allows modeling groups to modify their modern land/sea mask to the extent practical for their model, specifying, for example, West Antarctica as land. We use the “alternate” configuration for the CCSM4 PlioMIP simulation.

Simulating the mid-Pliocene Warm Period with the CCSM4 model

N. A. Rosenbloom et al.

Title Page

Abstract

Introduction

Conclusions

References

Tables

Figures



Back

Close

Full Screen / Esc

Printer-friendly Version

Interactive Discussion



3.1 CCSM4 initialization

We initialized the mPWP experiment from a long CCSM4 1850 preindustrial (PI) control simulation that was run to approximate equilibrium in accordance with CMIP5 (Coupled Model Intercomparison Project Phase 5) protocols. The PI control simulated 1300 model years with constant CO₂ (284.7 ppm), N₂O (275.68 ppb), and CH₄ (791.6 ppb), fixed incoming solar radiation at the top of the atmosphere (1360.9 W m⁻²) and prescribed aerosols (black and organic carbon, sulfate, dust and sea-salt). We branched from the PI control simulation at model year 801, running our mPWP simulation with the fully coupled CCSM4 model for 500 simulated years on Bluefire, an IBM Power6 computer located at the National Center for Atmospheric Research (NCAR) in Boulder, Colorado. The forcings and boundary conditions for the mPWP simulation are discussed below and summarized in Table 2.

3.2 Land-sea mask

In the mPWP the continents were very close their current locations, allowing us to use the modern CCSM4 land/sea mask for most of the globe. We modify the modern land/sea mask to remove Hudson Bay, a modern epicontinental sea formed by excavation and deformation of the Canadian Shield under the weight of Pleistocene ice (Fig. 1). As for our preindustrial control simulation, the Central American Seaway (Panama Gateway) is closed; modern ocean gateways, including the Bering Strait, Drake Passage, Tasman Gateway, Gibraltar Strait, and the Indonesian Gateway, remain open.

3.3 Topography and river routing

We create the mid-Pliocene topography by adding the PRISM3 topographic anomaly (mPWP minus modern) (Sohl et al., 2009; Amante and Eakins, 2008) to the CCSM4 modern topography. Implicit in the PRISM3 topographic anomaly is a 25 m increase

Simulating the mid-Pliocene Warm Period with the CCSM4 model

N. A. Rosenbloom et al.

[Title Page](#)

[Abstract](#)

[Introduction](#)

[Conclusions](#)

[References](#)

[Tables](#)

[Figures](#)



[Back](#)

[Close](#)

[Full Screen / Esc](#)

[Printer-friendly Version](#)

[Interactive Discussion](#)



in mean sea level, which we implement in CCSM4 without changing global coast-
lines. The largest changes in elevation are over Greenland and West Antarctica where
PRISM3 reduces the volume of continental ice sheets to reflect the 25 m sea level
change. Local elevation adjustments also affect the North American Rocky Mountains,
the Middle East and Asia. Minor georeferencing discrepancies between the PRISM3
and the CCSM4 base projections are evident in the North American Rocky Mountains
and in the Himalaya (Fig. 1). Following PlioMIP protocol (Haywood et al., 2011) we
set Hudson Bay and West Antarctica to 25 m above sea level. River discharge in the
mPWP simulation remains unchanged from present day; drainage across West Antarc-
tica and across land cells in the emergent Hudson Bay region is routed automatically
to the nearest ocean grid cell.

3.4 Vegetation

The PRISM3 data set defines global vegetation using the BIOME4 (Salzmann et al.,
2008, 2009) model reconstruction of mid-Pliocene plant biome communities. The Com-
munity Land Model (CLM4) uses plant functional types (PFTs) to describe vegetation
distributions (Oleson and Bonan, 2000; Bonan et al., 2002). To translate the BIOME4
plant biomes to analogous CLM4 plant functional types, we first spatially correlate
the modern BIOME4 biome communities to the modern CLM4/PFT landcover distri-
bution. Using the correlations developed from the modern biome-to-PFT comparison,
we spatially extrapolate the CLM4/PFTs to the BIOME4 Pliocene biome reconstruc-
tion, creating a new Pliocene PFT reconstruction for CLM4 that preserves the spa-
tial consistency of modern BIOME4-to-CLM4/PFT biogeography (see Lawrence and
Chase, 2010). This method has the advantage of retaining a physical connection to
present day PFT mapping. Soil type distributions are identical to preindustrial. To ini-
tialize the land model we project the CLM4 initial state from model year 801 of the
1300 yr PI control onto the modified mPWP land/sea mask.

Simulating the mid-Pliocene Warm Period with the CCSM4 model

N. A. Rosenbloom et al.

[Title Page](#)

[Abstract](#)

[Introduction](#)

[Conclusions](#)

[References](#)

[Tables](#)

[Figures](#)



[Back](#)

[Close](#)

[Full Screen / Esc](#)

[Printer-friendly Version](#)

[Interactive Discussion](#)



3.5 Land ice

The Greenland land ice reconstruction for the mPWP (Hill et al., 2007) greatly reduces the extent of the Greenland Ice Sheet (Fig. 1). In the SH, PRISM3 reconstructions suggest the WAIS was absent and the East Antarctic Ice Sheet (EAIS) was diminished during the mid-Pliocene. Although the “preferred” PlioMIP experimental boundary condition removes the WAIS and replaces it with ocean, we use the “alternate” protocol and instead lower the WAIS to 25 m to simulate removal of continental ice. We chose the “alternate” configuration package to avoid extensive modifications to the CCSM4 POP2 ocean grid and bathymetry near the WAIS. We replace land ice with shrubs and arctic grasses over the deglaciated areas of Greenland, WAIS, and EAIS, as prescribed by the BIOME4 plant biome reconstruction (Salzmann et al., 2008).

3.6 Initial ocean temperatures

We modify the initial temperature state of the full ocean using PRISM3 reconstructed deep ocean temperature anomalies (Haywood et al., 2011; Dowsett et al., 2009) in a process analogous to that used to create mPWP topography. We first create a deep ocean temperature (DOT) anomaly by differencing the PRISM3 ocean temperature reconstruction against modern day Levitus (mPWP minus Levitus) (Levitus and Boyer, 1994). We then interpolate the reconstructed DOT anomaly from its native $4^\circ \times 5^\circ$ latitude/longitude grid to the CCSM4 POP2 grid (384×320 grid cells), and remap the DOT anomaly from 33 layers to the 60 ocean levels used by POP2, before adding the DOT anomaly to year 801 of the preindustrial control simulation. To avoid numerical instabilities from restarting the ocean with a modified land/sea mask, we set velocities and surface pressure gradients to zero in the ocean initial files.

Simulating the mid-Pliocene Warm Period with the CCSM4 model

N. A. Rosenbloom et al.

[Title Page](#)

[Abstract](#)

[Introduction](#)

[Conclusions](#)

[References](#)

[Tables](#)

[Figures](#)



[Back](#)

[Close](#)

[Full Screen / Esc](#)

[Printer-friendly Version](#)

[Interactive Discussion](#)



4 Results

4.1 Approach to equilibrium

Global averaged mean annual air temperature (Fig. 2a) warms for the first 140 yr of the simulation, stabilizing, after a small overshoot, by year 180 at 15.9°C, 1.9°C warmer than the PI control. The initial ocean response was strongly affected by the warm DOT anomaly applied to the full ocean. The result was a reduction of the Atlantic Meridional Overturning Circulation (AMOC), which immediately decreased from an initial strength of 24 Sv to 17 Sv (Fig. 2b). The overturning circulation recovered within 135 model years, weakly overshooting to a maximum of 28 Sv before stabilizing at 26 Sv, similar to the preindustrial CCSM4 AMOC strength. Globally averaged ocean temperature continues to warm by ~0.025°C per century (Fig. 2c), which is similar in magnitude, although opposite in sign, to the PI control simulation, and indicates that the deep ocean is still coming into equilibrium, a process that takes thousands of years.

4.2 Surface air temperature

Simulated annual and seasonal air temperatures demonstrate warming globally (Fig. 3) relative to the preindustrial control (stippling indicates results are not statistically significant at 95%). Globally averaged mean annual temperature (MAT) increases by 1.9°C (Table 2) with enhanced warming over land (2.6°C) relative to oceans. Zonally averaged MAT increases > 5°C at high latitudes, while tropical MAT warms by only ~1°C. Seasonal warming at high latitudes is such that zonally averaged boreal and austral wintertime temperatures increase by ~6°C while summertime temperatures warm by only ~2°C. High latitude warming is greater in the NH.

Fine-scale temperature variability across North America and Asia is caused by differences between the PRISM3 and CCSM4 base projections (Fig. 1). Surface warming over East Antarctic reflects the reduced profile of the EAIS during the mPWP (Fig. 1), while warming over Greenland and West Antarctica reflects the dual effects of lowered

Simulating the mid-Pliocene Warm Period with the CCSM4 model

N. A. Rosenbloom et al.

[Title Page](#)

[Abstract](#)

[Introduction](#)

[Conclusions](#)

[References](#)

[Tables](#)

[Figures](#)



[Back](#)

[Close](#)

[Full Screen / Esc](#)

[Printer-friendly Version](#)

[Interactive Discussion](#)



elevation and landcover conversion from land ice to arctic grasses. The northward expansion of broadleaf and needleleaf trees in BIOME4 and consequent lowering of surface albedo contributes to wintertime warming across northeastern Siberia (Fig. 3c). Relative wintertime cooling across southern Siberia is similarly related to a conversion from forests to grassland, with a consequent increase in surface albedo. Relative warming and cooling over Hudson Bay is the result of the land/sea mask conversion from ocean to land.

4.3 Precipitation

Globally averaged mean precipitation increased slightly ($0.086 \text{ mm day}^{-1}$) in the mid-Pliocene experiment, with a relatively greater increase over land ($0.093 \text{ mm day}^{-1}$) (Table 2). Figure 4 shows annual and seasonal precipitation change. The pattern of seasonal precipitation indicates a northward shift of the Intertropical Convergence Zone (ITCZ) in response to enhanced NH warming of subtropical SSTs (Fig. 5). Boreal summer precipitation (June-July-August; JJA) increases by $> 2 \text{ mm day}^{-1}$ in the eastern equatorial Pacific Basin, the Arabian and Solomon Seas, and the monsoon regions of northern Africa and India. JJA precipitation falls by -1 mm day^{-1} over Siberia and parts of North and South America. Precipitation increases significantly in austral summer (December-January-February; DJF) as monsoons increase precipitation by 1.5 mm day^{-1} over equatorial Africa, the Bay of Bombay, South China Sea, and Papua New Guinea and the Amazon monsoon region. DJF rainfall decreases by 2 to 4 mm day^{-1} over the Brazilian Highlands.

4.4 Sea surface temperature and salinity

In the North Pacific, CCSM4 SST warms by 2 to 4°C ; proxy indicators suggest 0 to 4°C change along the eastern and southern Aleutian Islands and up to $\sim 6^\circ\text{C}$ warming off the west coast of North America (Fig. 5). The model correctly captures warming (1 to 2°C) in the eastern equatorial Pacific Basin, but falls short of the 2 to 4°C warming

Simulating the mid-Pliocene Warm Period with the CCSM4 model

N. A. Rosenbloom et al.

[Title Page](#)

[Abstract](#)

[Introduction](#)

[Conclusions](#)

[References](#)

[Tables](#)

[Figures](#)



[Back](#)

[Close](#)

[Full Screen / Esc](#)

[Printer-friendly Version](#)

[Interactive Discussion](#)



Simulating the mid-Pliocene Warm Period with the CCSM4 model

N. A. Rosenbloom et al.

[Title Page](#)

[Abstract](#)

[Introduction](#)

[Conclusions](#)

[References](#)

[Tables](#)

[Figures](#)

[⏪](#)

[⏩](#)

[◀](#)

[▶](#)

[Back](#)

[Close](#)

[Full Screen / Esc](#)

[Printer-friendly Version](#)

[Interactive Discussion](#)

indicated by proxy reconstructions in the equatorial upwelling region. Similarly, the model correctly replicates the sign but not the magnitude of warming seen in proxy records along the northwest coast of Africa. CCSM4 warming in the western Pacific of 2 to 4 °C compares well with reconstructed records east of the Kamchatka Peninsula, but falls short of the 4 to 6 °C of warming indicated further south off the Kuril Islands. CCSM4 SSTs in the North Atlantic warm by 2 to 4 °C near the southern tip of Greenland, but do not capture the >10 °C of warming suggested by proxy reconstructions. Two limited regions in the North Atlantic cool by 1 to 2 °C in CCSM4. Proxy reconstructions in the Southern Ocean show regional heterogeneity with some proxies signaling ~ 1 °C cooling, and other areas pointing to as much as 3 °C warming. CCSM4 temperatures in the Southern Ocean warm by 2 to 4 °C in the South Atlantic and Indian Ocean sectors. Simulated temperatures in the South Pacific increase by < 2 °C.

Sea surface salinity (Fig. 6) indicates widespread freshening in the polar oceans, where contraction in thickness and extent of sea ice in the mPWP simulation signals an overall reduction in brine rejection, and a consequent fall in sea surface salinity relative to preindustrial. A low salinity plume from the Labrador Sea is carried southward by the Labrador Current, entrained off the coast of Newfoundland and carried east and south along the northern edge of the North Atlantic Drift. Conversely, an increase in the evaporation minus precipitation (E-P) in the tropical Atlantic Ocean and mid-latitude North Pacific Ocean results in saltier Gulf Stream and East Pacific Currents. Increased tropical precipitation and runoff off Southeast Asia lower sea surface salinity from the South China Sea and the Bay of Bengal to the Arafura Sea and the north coast of Australia. Increased runoff from the Pacific Northwest in North America lowers salinity in the Gulf of Alaska.

4.5 Ocean circulation

The simulated mPWP AMOC is comparable to the PI control (Fig. 7a, b). Positive/negative stream function strength indicates clockwise/counterclockwise flow; clockwise flow in the North Atlantic tracks the northward cycling of warm surface water;

counterclockwise flow tracks northward flowing deep water from the Southern Ocean. In the mPWP simulation Southern Ocean water is moving with roughly similar velocity and strength as in the preindustrial simulation. However, Southern Ocean flow moves much farther north in the mPWP simulation with Antarctic Bottom Water filling the deep basin up to sill depth.

Northward ocean heat transport in the Atlantic Basin for the simulated mPWP (Fig. 7c) is indistinguishable from preindustrial. This unremarkable response is likely a factor in why the model does not capture the magnitude of warming indicated by North Atlantic temperature proxies. Simulated NH SSTs do not warm enough in the mPWP, particularly in the North Atlantic, whereas SH SSTs are too warm, suggesting that enhanced northward ocean heat transport might redistribute enough ocean heat to bring CCSM4 SSTs more in line with proxy evidence.

4.6 Sea ice

Mid-Pliocene sea ice extent [areal %] and thickness fall in both hemispheres (Fig. 8). Overall summertime sea ice extent is reduced by $\sim 23\%$ in the Arctic, particularly along the coastal continental shelf, as well as in the Labrador, Greenland and Norwegian Seas where areal extent is reduced by $> 25\%$ (Fig. 8). Wintertime sea ice extent (not shown) is reduced by a modest 4% across the Arctic, but drops dramatically in the Pacific Basin where spatial maps indicate a $> 20\%$ reduction in the Bering Sea and the Sea of Okhotsk. Similar declines are seen in the Barents Sea, off the southeast coast of Greenland, and in the Labrador Sea along the coast of Newfoundland. Winter and summertime sea ice thickness is reduced by as much as 2 m across the Arctic, with even greater thinning (2 to 4 m) off the northern coasts of Greenland and the Queen Elizabeth Islands. Wintertime sea ice thins by up to a meter in the Bering Sea and Sea of Okhotsk, and in the Labrador Sea south to Newfoundland. The PRISM3 sea ice reconstruction (Dowsett, 2007; Robinson, 2008; Dowsett and Robinson, 2009) used by the PlioMIP AGCM Experiment 1 (Haywood, 2010) prescribes an ice-free Arctic Ocean

Simulating the mid-Pliocene Warm Period with the CCSM4 model

N. A. Rosenbloom et al.

[Title Page](#)

[Abstract](#)

[Introduction](#)

[Conclusions](#)

[References](#)

[Tables](#)

[Figures](#)



[Back](#)

[Close](#)

[Full Screen / Esc](#)

[Printer-friendly Version](#)

[Interactive Discussion](#)



during boreal summer. The CCSM4 simulation of the mid-Pliocene shows diminished but persistent seasonal sea ice cover for July-August-September.

In the SH, average summertime sea ice extent around Antarctica falls by $\sim 30\%$. Regionally, summer sea ice extent increases slightly ($< 5\%$) in the Weddell Sea and in isolated pockets of the Ross and Bellingshausen Seas and in Prydz Bay (5 to 15%). Wintertime sea ice extent increases by up to 10% in these same areas, but falls by more than 30% within the distal third of the seasonal ice pack. Both summer and wintertime sea ice thins by ~ 1.2 m close to the continent and by 0.4 to 0.8 m across the edge of the Ronne Ice Shelf in the Weddell Sea, along the west coast of the Antarctic Peninsula, the eastern coast of the Ross Sea and along the edge of the Amery Ice Shelf in Prydz Bay.

4.7 ENSO

The mPWP simulation of Nino3.4 is similar to the preindustrial control in seasonal cycle and dominant 3 to 6 yr periodicity. However the Nino3.4, estimated over the last 300 yr of the mPWP, is roughly 20% weaker ($\sigma = 0.82$) compared to the PI ($\sigma = 1.01$), with extended periods of quiescence of up to 150 yr (Fig. 9) compared to similar intervals with only half the duration in the preindustrial. The model does simulate mPWP warming in the eastern equatorial Pacific Basin, signaling a relaxation of the zonal SST gradient similar to the response found in the CCSM4 abrupt $4 \times \text{CO}_2$ simulation (Brady et al., 2012), which also has a weakened Nino3.4 ($\sigma = 0.75$).

5 Comparison to data

Temperature reconstructions indicate that globally averaged mean annual air temperature (MAT) was 2 to 3°C warmer during the Pliocene and as much as 15 to 20°C warmer at high latitudes, particularly the Arctic (Ballantyne, 2010). In our CCSM4

Simulating the mid-Pliocene Warm Period with the CCSM4 model

N. A. Rosenbloom et al.

Title Page

Abstract

Introduction

Conclusions

References

Tables

Figures

⏪

⏩

◀

▶

Back

Close

Full Screen / Esc

Printer-friendly Version

Interactive Discussion



mPWP simulation, globally averaged mPWP surface temperatures increase by 1.9°C relative to preindustrial (Table 2), comparing favorably with the reconstructed global average. However, simulated temperatures are conspicuously at odds with proxy records in several critical areas when we plot proxy data against corresponding CCSM4 annual temperatures from the nearest latitude/longitude grid cell, and partition the results by region. Figure 10 shows that in general CCSM4 overestimates warming in the Southern Hemisphere extratropics by 1 to 4°C. Conversely, CCSM4 temperatures in the NH extratropics fail to capture the extent of warming expected, particularly in the North Atlantic, where proxy estimates exceed model temperatures by as much as 7°C. The model shows a uniform increase of ~1°C in the tropics but does not capture the 2 to 4°C of warming indicated by proxy reconstructions. The lack of increase in northward ocean heat transport in the Atlantic basin (Fig. 7) is consistent with the weaker than expected temperature response in the North Atlantic and warmer than expected SSTs in the Southern Hemisphere.

6 Relevance to future projections

Proxy temperature reconstructions from the Pliocene Arctic point to a reduced equator to pole temperature gradient. In Fig. 11 we plot the polar amplification, which is the zonally-averaged mean annual surface temperature change for the mid-Pliocene simulation normalized by the global mean annual temperature change for the same period. We show the mPWP response together with the results from a CCSM4 CO₂ sensitivity simulation where CO₂ was abruptly elevated to four times the preindustrial CO₂ concentration (4 × CO₂). The forcing for the mPWP includes changes to the land/sea mask over Hudson Bay, changes to the size and extent of the Greenland and Antarctic Ice Sheets, and widespread vegetation shifts, along with an estimated radiative forcing of 1.9 W m⁻² from elevated CO₂. The 4 × CO₂ simulation has an estimated radiative forcing from CO₂ alone of 7.4 W m⁻², relative to the PI. The mPWP simulation has a comparable latitudinal response to the CCSM4 4 × CO₂ experiment; both simulations show a muted

Simulating the mid-Pliocene Warm Period with the CCSM4 model

N. A. Rosenbloom et al.

[Title Page](#)

[Abstract](#)

[Introduction](#)

[Conclusions](#)

[References](#)

[Tables](#)

[Figures](#)



[Back](#)

[Close](#)

[Full Screen / Esc](#)

[Printer-friendly Version](#)

[Interactive Discussion](#)



tropical response, with polar amplification of ~ 3 times the global temperature change. The exaggerated warming/cooling signal in the mPWP SH temperature is caused by the removal of the WAIS and lowering of the EAIS.

We compare mPWP Arctic sea ice concentration against the CCSM4 CMIP5 RCP2.6 simulation (radiative forcing = 2.6 W m^{-2}) in Fig. 12. We show the RCP2.6 ensemble member with the greatest reduction in NH sea ice extent, and compare years 2080–2099 from RCP2.6 against years 1980–1999 from the end of the 20th century simulation. Arctic sea ice reduction is greater in the mPWP simulation (relative to the PI control), than in the RCP2.6 simulation (relative to the end of the 20th century).

7 Summary

We present results from a 500 yr simulation of the mPWP using the CCSM4 fully coupled model as part of the PlioMIP. The mPWP was the last prolonged period in Earth history when CO_2 concentrations were similar to present day, resulting in global mean temperatures that were 2 to 3°C warmer than modern and polar temperatures that were as much as 20°C warmer. The experimental design for the CCSM4 simulation follows the “alternate” PlioMIP protocol for Experiment 2. Results from the CCSM4 simulation show a 1.9°C increase in globally averaged mean annual surface temperature relative to the CCSM4 1850 PI control, with zonally averaged temperature increases of 6°C at high latitudes and polar amplification of ~ 3 times the global warming. High latitude warming is greater in the NH than SH. Average surface temperature over land increases by 2.4°C ; globally averaged sea surface temperature increases by 1.2°C . Global precipitation increases slightly by 0.09 mm day^{-1} and the ITCZ shifts northward reflecting greater warming in NH SSTs. Areal sea ice extent decreases in both hemispheres, with a greater decrease in the Southern Hemisphere. Arctic sea ice in CCSM4 thins by $> 2 \text{ m}$ but persists through boreal summer (JAS). The model correctly captures warming in the eastern Pacific Basin signaling a relaxation of the zonal SST gradient, but fails to capture the magnitude of warming in equatorial upwelling areas. Northward

Simulating the mid-Pliocene Warm Period with the CCSM4 model

N. A. Rosenbloom et al.

Title Page

Abstract

Introduction

Conclusions

References

Tables

Figures

⏪

⏩

◀

▶

Back

Close

Full Screen / Esc

Printer-friendly Version

Interactive Discussion



ocean heat transport in the Atlantic Basin is indistinguishable from the control. CCSM4 produces weaker warming than expected in the North Atlantic, and greater warming than expected in the Southern Hemisphere. This bipolar bias suggests an increase in northward oceanic heat transport could bring CCSM4 into better agreement with SST reconstructions.

Acknowledgements. We thank the PRISM group for providing the mid-Pliocene datasets for PlioMIP. We also thank the large community of scientists and engineers who contribute to the development of CCSM. The CESM project is supported by the National Science Foundation and the Department of Energy. Computing resources were provided by the Climate Simulation Laboratory (CSL) at NCAR's Computational and Information Systems Laboratory (CISL), which is sponsored by the National Science Foundation and other agencies. This research was enabled by CISL compute and storage resources. Bluefire, a 4064-processor IBM Power6 resource with a peak of 77 TeraFLOPS provided more than 7.5 million computing hours, the GLADE high-speed disk resources provided 0.4 petabytes of dedicated disk, and CISL's 12-PB HPSS archive provided over 1 petabyte of storage in support of this research project.

References

- Amante, C. and Eakins, B. W.: ETOPO1 1 Arc-Minute Global Relief Model: Procedures, Data Sources and Analysis, National Geophysical Data Center, NESDIS, NOAA, US Department of Commerce, Boulder, CO, 2008.
- Ballantyne, A. P., Greenwood, D. R., Sinninghe Damste, J. S., Czank, A. Z., Eberle, J. J., and Rycbynski, N.: Significantly warmer Arctic surface temperatures during the Pliocene indicated by multiple independent proxies, *Geology*, 38, 603–606, 2010.
- Bonan, G. B., Levis, S., Kergoat, L., and Oleson, K. W.: Landscapes as patches of plant functional types: An integrating concept for climate and ecosystem models, *Global Biogeochem. Cy.*, 16, 1021, 23 pp., doi:10.1029/2000GB001360, 2002.
- Brady, E. C., Otto-Bliesner, B. L., Kay, J. E., and Rosenbloom, N. A.: Sensitivity to Glacial Forcing in the CCSM4, *J. Climate*, doi:10.1175/JCLI-D-11-00416.1, special issue, accepted, 2012.

Simulating the mid-Pliocene Warm Period with the CCSM4 model

N. A. Rosenbloom et al.

Title Page

Abstract

Introduction

Conclusions

References

Tables

Figures



Back

Close

Full Screen / Esc

Printer-friendly Version

Interactive Discussion



Simulating the mid-Pliocene Warm Period with the CCSM4 model

N. A. Rosenbloom et al.

[Title Page](#)

[Abstract](#)

[Introduction](#)

[Conclusions](#)

[References](#)

[Tables](#)

[Figures](#)

⏪

⏩

◀

▶

[Back](#)

[Close](#)

[Full Screen / Esc](#)

[Printer-friendly Version](#)

[Interactive Discussion](#)



- Branstetter, M. L. and Famiglietti, J. S.: Testing the sensitivity of GCM-simulated runoff to climate model resolution using a parallel river transport algorithm, Preprints, 14th Conference on Hydrology, Dallas, TX, Amer. Meteor. Soc., 6B.11, 1999.
- Briegleb, B. P., Danabasoglu, G., and Large, W. G.: An overflow parameterization for the ocean component of the Community Climate System Model. NCAR Tech, Note NCAR/ TN-4811STR, 72 pp., 2010.
- Danabasoglu, G., Large, W. G., Tribbia, J. J., Gent, P. R., Briegleb, B. P., and McWilliams, J. C.: Diurnal coupling in the tropical oceans of CCSM3, *J. Climate*, 19, 2347–2365, 2006.
- Danabasoglu, G., Large, W. G., and Briegleb, B. P.: Climate impacts of parameterized Nordic Sea overflows, *J. Geophys. Res.*, 115, C11005, doi:10.1029/2010JC006243, 2010.
- Danabasoglu, G., Bates, S. C., Briegleb, B. P., Jayne, S. R., Jochum, M., Large, W. G., Peacock, S., and Yeager, S. G.: The CCSM4 Ocean Component, *J. Climate*, 25, 1361–1389, 2012.
- Deser, C., Phillips, A. S., Tomas, R. A., Okumura, Y. M., Alexander, M. A., Capotondi, A., and Scott, J. D.: ENSO and Pacific Decadal Variability in the Community Climate System Model Version 4, *J. Climate*, 25, 2622–2651, 2012.
- Dowsett, H. J.: Faunal re-evaluation of Mid-Pliocene conditions in the western equatorial Pacific, *Micropaleontology*, 53, 447–456, 2007.
- Dowsett, H. J.: The PRISM palaeoclimate reconstruction and Pliocene sea-surface temperature, in: *Deep-time perspectives on climate change: Marrying the signal from computer models and biological proxies*, edited by: Williams, M., Haywood, A. M., Gregory, J., and Schmidt, D. N., *Micropalaeontological Soc., Spec. Pub., Geol. Soc. of London*, London, UK, 459–480, 2007.
- Dowsett, H. J. and Robinson, M. M.: Mid-Pliocene equatorial Pacific sea surface temperature reconstruction: a multi-proxy perspective, *Philos. T. R. Soc. A*, 367, 109–126, 2009.
- Dowsett, H. J., Robinson, M. M., and Foley, K. M.: Pliocene three-dimensional global ocean temperature reconstruction, *Clim. Past*, 5, 769–783, doi:10.5194/cp-5-769-2009, 2009.
- Dowsett, H. J., Robinson, M. M., Stoll, D. K., and Foley, K. M.: Mid-Piacenzian mean annual sea surface temperature analysis for data-model comparisons, *Stratigraphy*, 7, 189–198, 2010.
- Gent, P. R., Danabasoglu, G., Donner, L. J., Holland, M. M., Hunke, E. C., Jayne, S. R., Lawrence, D. M., Neale, R. B., Rasch, P. J., Vertenstein, M., Worley, P. H., Yang, Z.-L., and Zhang, M.: The Community Climate System Model Version 4, *J. Climate*, 24, 4973–4991, 2011.

Simulating the mid-Pliocene Warm Period with the CCSM4 model

N. A. Rosenbloom et al.

[Title Page](#)

[Abstract](#)

[Introduction](#)

[Conclusions](#)

[References](#)

[Tables](#)

[Figures](#)

⏪

⏩

◀

▶

[Back](#)

[Close](#)

[Full Screen / Esc](#)

[Printer-friendly Version](#)

[Interactive Discussion](#)



- Haywood, A. M., Dowsett, H. J., Otto-Bliesner, B., Chandler, M. A., Dolan, A. M., Hill, D. J., Lunt, D. J., Robinson, M. M., Rosenbloom, N., Salzmann, U., and Sohl, L. E.: Pliocene Model Inter-comparison Project (PlioMIP): experimental design and boundary conditions (Experiment 1), *Geosci. Model Dev.*, 3, 227–242, doi:10.5194/gmd-3-227-2010, 2010.
- 5 Haywood, A. M., Dowsett, H. J., Robinson, M. M., Stoll, D. K., Dolan, A. M., Lunt, D. J., Otto-Bliesner, B., and Chandler, M. A.: Pliocene Model Intercomparison Project (PlioMIP): experimental design and boundary conditions (Experiment 2), *Geosci. Model Dev.*, 4, 571–577, doi:10.5194/gmd-4-571-2011, 2011.
- Hill, D. J., Haywood, A. M., Hindmarsh, R. C. A., and Valdes, P. J.: Characterising ice sheets during the mid Pliocene: evidence from data and models, in: *Deep time perspectives on climate change, Marrying the signal from computer models and biological proxies*, edited by: Williams, M., Haywood, A. M., Gregory, F. J., and Schmidt, D. N., the Micropalaeontological Society, Special Publications, the Geological Society, London, 517–538, 2007.
- 10 Holland, M. M., Bailey, D. A., Briegleb, B. P., Light, B., and Hunke, E.: Improved Sea Ice Shortwave Radiation Physics in CCSM4: The Impact of Melt Ponds and Aerosols on Arctic Sea Ice*, *J. Climate*, 25, 1413–1430, doi:10.1175/JCLI-D-11-00078.1, 2012.
- Hunke, E. and Lipscomb, W. H.: CICE: The Los Alamos sea ice model, documentation and software, version 4.0, Los Alamos National Laboratory Tech. Rep. LA-CC-06-012, 76 pp., 2008.
- 20 Jahn, A., Bailey, D. A., Bitz, C. M., Holland, M. M., Hunke, E. C., Kay, J. E., Lipscomb, W. H., Maslanik, J. A., Pollak, D., Sterling, K., and Strøve, J.: Late 20th Century Simulation of Arctic Sea Ice and Ocean Properties in the CCSM4, *J. Climate*, 25, 1431–1452, doi:10.1175/JCLI-D-11-00201.1, 2012.
- Jochum, M., Danabasoglu, G., Holland, M. M., Kwon, Y.-O., and Large, W. G.: Ocean viscosity and climate, *J. Geophys. Res.*, 113, C06017, doi:10.1029/2007JC004515, 2008.
- 25 Kay, J. E., Hillman, B. R., Klein, S. A., Zhang, Y., Medeiros, B., Pincus, R., Gettelman, A., Eaton, B., Boyle, J., Marchand, R., and Ackerman, T. P.: Exposing Global Cloud Biases in the Community Atmosphere Model (CAM) Using Satellite Observations and Their Corresponding Instrument Simulators, *J. Climate*, 25, 5190–5207, 2012a.
- 30 Kay, J. E., Holland, M. M., Bitz, C. M., Blanchard-Wrigglesworth, E., Gettelman, A., Conley, A., and Bailey, D.: The Influence of Local Feedbacks and Northward Heat Transport on the Equilibrium Arctic Climate Response to Increased Greenhouse Gas Forcing, *J. Climate*, 25, 5433–5450, 2012b.

Sohl, L. E., Chandler, M. A., Schmunk, R. B., Mankoff, K., Jonas, J. A., Foley, K. M., and Dowsett, H. J.: PRISM3/GISS topographic reconstruction, US Geological Survey Data Series, 419, p. 6, 2009.

5 Smith, R., Jones, P., Briegleb, B., Bryan, F., Danabasoglu, G., Dennis, J., Dukowicz, J., Eden, C., Fox-Kemper, B., Gent, P., Hecht, M., Jayne, S., Jochum, M., Large, W., Lindsay, K., Maltrud, M., Norton, N., Peacock, S., Vertenstein, M., and Yeager, S.: The Parallel Ocean Program (POP) reference manual, ocean component of the Community Climate System Model (CCSM), Los Alamos National Laboratory Tech. Rep. LAUR-10-01853, 141 pp., 2010.

GMDD

5, 4269–4303, 2012

Simulating the mid-Pliocene Warm Period with the CCSM4 model

N. A. Rosenbloom et al.

Title Page

Abstract

Introduction

Conclusions

References

Tables

Figures



Back

Close

Full Screen / Esc

Printer-friendly Version

Interactive Discussion



Table 1. Summary of forcings and boundary conditions for the mid-Pliocene and 1850 preindustrial control simulations.

	PI Control	Pliocene
Experimental design	CMIP5	PlioMIP Exp 2 Alternate
Land/sea mask	CCSM4 _{Modern}	CCSM4 _{Modern} – Hudson Bay
Resolution	1° ocn, ice, atm, Ind	1° ocn, ice, atm, Ind
Topography	CCSM4 _{Modern}	CCSM4 _{modern} + ΔPRISM3 BIOME4 converted to CLM4-
Landcover	CCSM4 _{Modern}	PFTs with PI control _{year,801} carbon pools
SST and deep ocean temperature (DOT)	PI control _{year,801}	1850 Control _{year,801} + Δ DOT _{PRISM3}
Ice sheets	CCSM4 _{Modern}	PRISM3 reductions to Greenland and Antarctic Ice Sheets
West Antarctic Ice Sheet (WAIS)	CCSM4 _{Modern}	WAIS replaced by vegetation at to 25 m above MSL.
Ocean bathymetry	CCSM4 _{Modern}	CCSM4 _{Modern}
Ocean gateways	CCSM4 _{Modern} CO ₂ = 284.7 ppm	CCSM4 _{Modern} CO ₂ = 405 ppm
Greenhouse gases	N ₂ O = 275.68 ppb CH ₄ = 791.6 ppb	N ₂ O = 275.68 ppb CH ₄ = 791.6 ppb
Solar constant	1360.89 W m ⁻²	1360.89 W m ⁻²
Orbital forcing	1990	1990
Aerosol flux	1850	1850
Simulation length	1300 y	500 y
Analysis years	1271–1300	471–500

Simulating the mid-Pliocene Warm Period with the CCSM4 model

N. A. Rosenbloom et al.

Title Page

Abstract

Introduction

Conclusions

References

Tables

Figures



Back

Close

Full Screen / Esc

Printer-friendly Version

Interactive Discussion



Simulating the mid-Pliocene Warm Period with the CCSM4 model

N. A. Rosenbloom et al.

Table 2. Summary of CCSM4 model response.

Variable	Pliocene	Change from PI
Global surface temperature (°C)	15.9	1.9
NH surface temperature (20N–90N) (°C)	11.1	2.3
SH surface temperature (90S–20S) (°C)	8.9	2.2
Surface temperature over land (°C)	9.6	2.4
Global precipitation (mm d ⁻¹)	3.0	0.086
Precipitation over land (mm d ⁻¹)	2.5	0.093
TOA energy imbalance (W m ²)	0.02	0.14
Sea surface salinity (psu)	34.21	-0.14
Sea surface temperature (°C)	21.6	1.2
NH Sea ice area (10 ⁶ km ²)	9.0	-2.7 (-23%)
SH Sea ice area (10 ⁶ km ²)	11.9	-5.1 (-30%)
Nino 3.4 σ	0.82	-0.19

Title Page

Abstract

Introduction

Conclusions

References

Tables

Figures



Back

Close

Full Screen / Esc

Printer-friendly Version

Interactive Discussion

Simulating the mid-Pliocene Warm Period with the CCSM4 model

N. A. Rosenbloom et al.

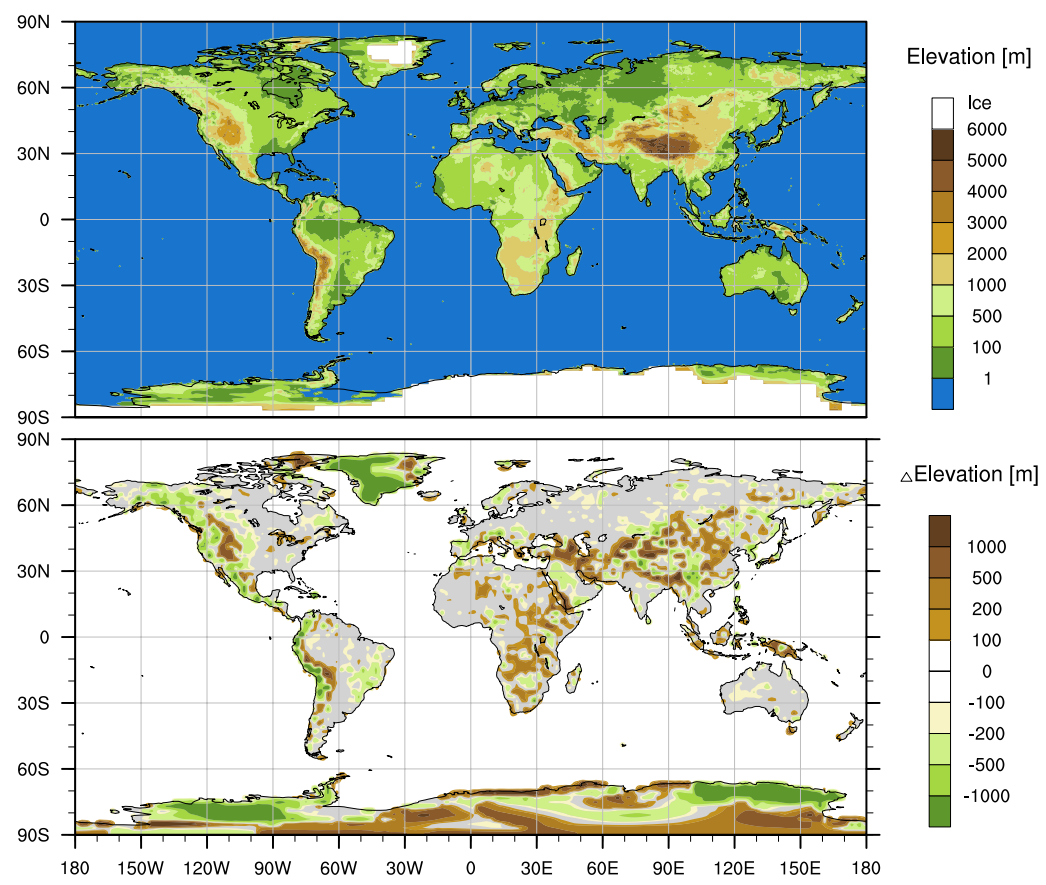


Fig. 1. CCSM4 implementation of PRISM3 land ice distribution and elevation map (top) and elevation anomaly (bottom).

[Title Page](#)
[Abstract](#) [Introduction](#)
[Conclusions](#) [References](#)
[Tables](#) [Figures](#)
⏪ ⏩
◀ ▶
[Back](#) [Close](#)
[Full Screen / Esc](#)
[Printer-friendly Version](#)
[Interactive Discussion](#)



**Simulating the
mid-Pliocene Warm
Period with the
CCSM4 model**

N. A. Rosenbloom et al.

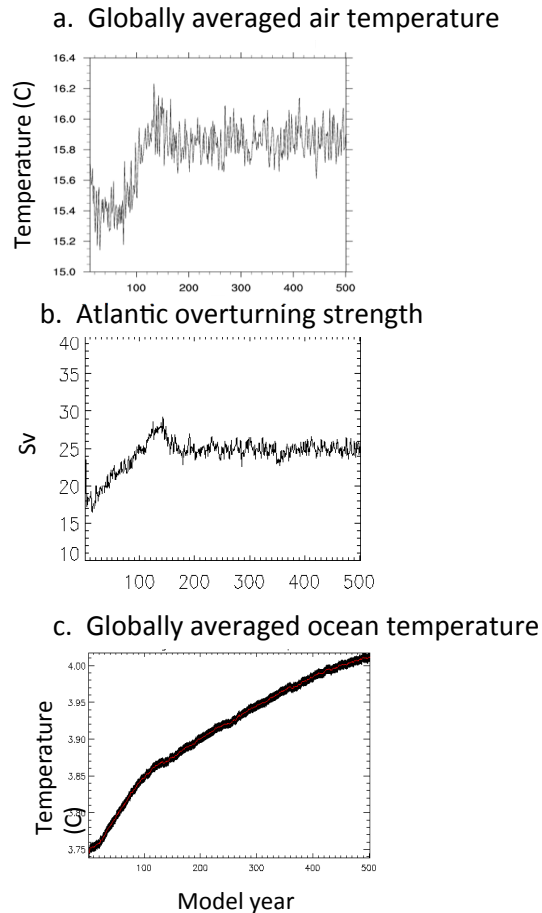


Fig. 2. Timeseries plots of simulated mPWP mean annual surface air temperature (top), globally averaged ocean temperature (middle), and Atlantic overturning strength (bottom).

[Title Page](#)[Abstract](#)[Introduction](#)[Conclusions](#)[References](#)[Tables](#)[Figures](#)[◀](#)[▶](#)[◀](#)[▶](#)[Back](#)[Close](#)[Full Screen / Esc](#)[Printer-friendly Version](#)[Interactive Discussion](#)

Simulating the mid-Pliocene Warm Period with the CCSM4 model

N. A. Rosenbloom et al.

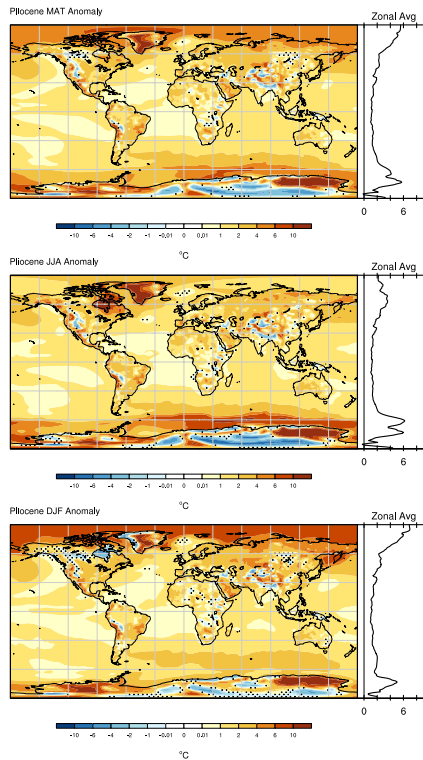


Fig. 3. CCSM4 simulated annual and seasonal Pliocene surface temperature change from PI control; stippling indicates results are not statistically significant at 95% level. Zonally averaged temperature change (mPWP minus control) is plotted in the side panels.

[Title Page](#)
[Abstract](#)
[Introduction](#)
[Conclusions](#)
[References](#)
[Tables](#)
[Figures](#)
[⏪](#)
[⏩](#)
[◀](#)
[▶](#)
[Back](#)
[Close](#)
[Full Screen / Esc](#)
[Printer-friendly Version](#)
[Interactive Discussion](#)

Simulating the mid-Pliocene Warm Period with the CCSM4 model

N. A. Rosenbloom et al.

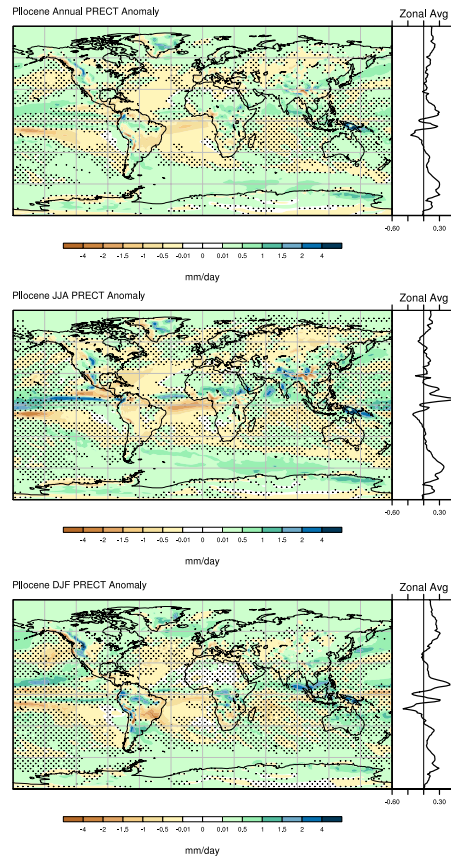


Fig. 4. CCSM4 simulated annual and seasonal Pliocene precipitation change from PI control; stippling indicates results are not statistically significant at 95 % level. Zonally averaged precipitation change (mPWP minus control) is plotted in the side panels.

Simulating the mid-Pliocene Warm Period with the CCSM4 model

N. A. Rosenbloom et al.

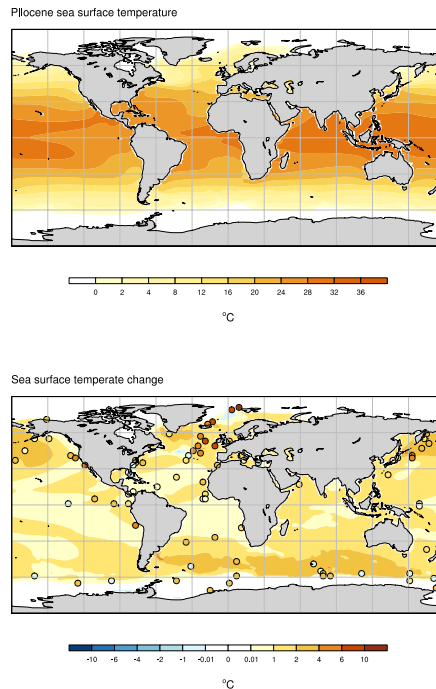


Fig. 5. CCSM4 simulated Pliocene sea surface temperature (top) and change from present day (bottom). White regions indicate sea ice in the mPWP simulation (top and both the mPWP and PI simulations (bottom)). Proxy data are plotted as open circles; color code indicates temperature change from present day.

[Title Page](#)[Abstract](#)[Introduction](#)[Conclusions](#)[References](#)[Tables](#)[Figures](#)[⏪](#)[⏩](#)[◀](#)[▶](#)[Back](#)[Close](#)[Full Screen / Esc](#)[Printer-friendly Version](#)[Interactive Discussion](#)

Simulating the mid-Pliocene Warm Period with the CCSM4 model

N. A. Rosenbloom et al.

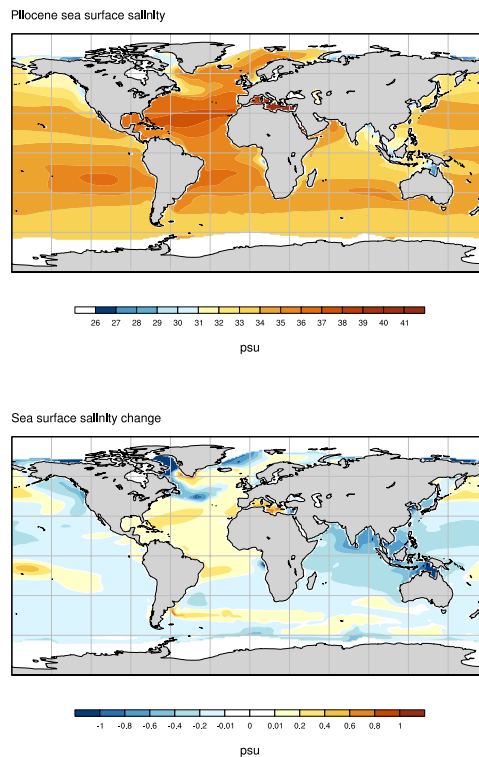


Fig. 6. Sea surface salinity (top) and change from PI control (bottom).

[Title Page](#)[Abstract](#)[Introduction](#)[Conclusions](#)[References](#)[Tables](#)[Figures](#)[⏪](#)[⏩](#)[◀](#)[▶](#)[Back](#)[Close](#)[Full Screen / Esc](#)[Printer-friendly Version](#)[Interactive Discussion](#)

Simulating the mid-Pliocene Warm Period with the CCSM4 model

N. A. Rosenbloom et al.

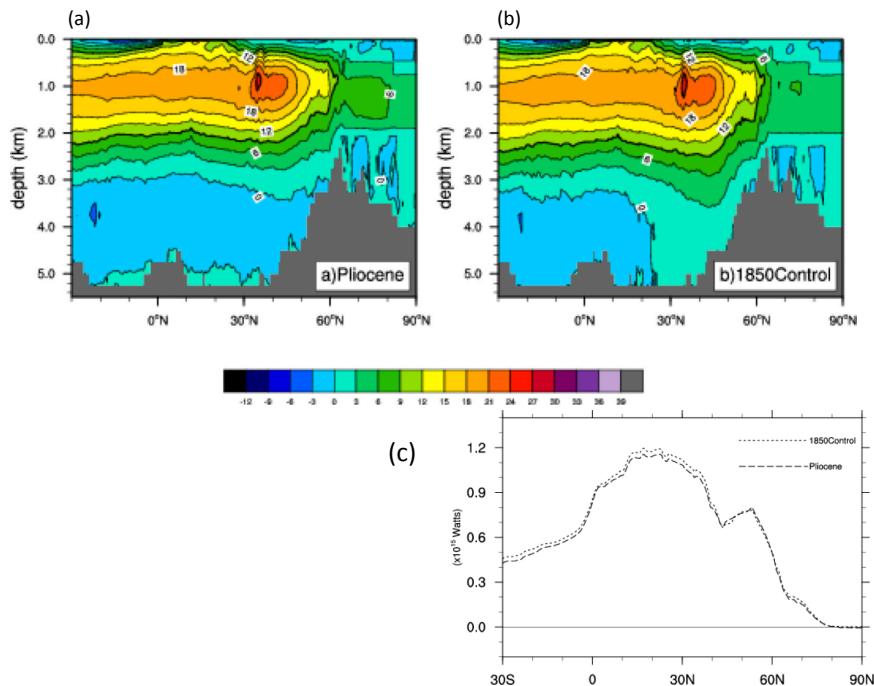


Fig. 7. Average annual eulerian mean Meridional Overturning Circulation in the Atlantic Ocean basin for the mPWP (a) and 1850 PI control (b). Northward ocean heat transport in the Atlantic Basin (c) for the mPWP (dashed) and the PI control (dotted).

[Title Page](#)

[Abstract](#)

[Introduction](#)

[Conclusions](#)

[References](#)

[Tables](#)

[Figures](#)

[⏪](#)

[⏩](#)

[◀](#)

[▶](#)

[Back](#)

[Close](#)

[Full Screen / Esc](#)

[Printer-friendly Version](#)

[Interactive Discussion](#)

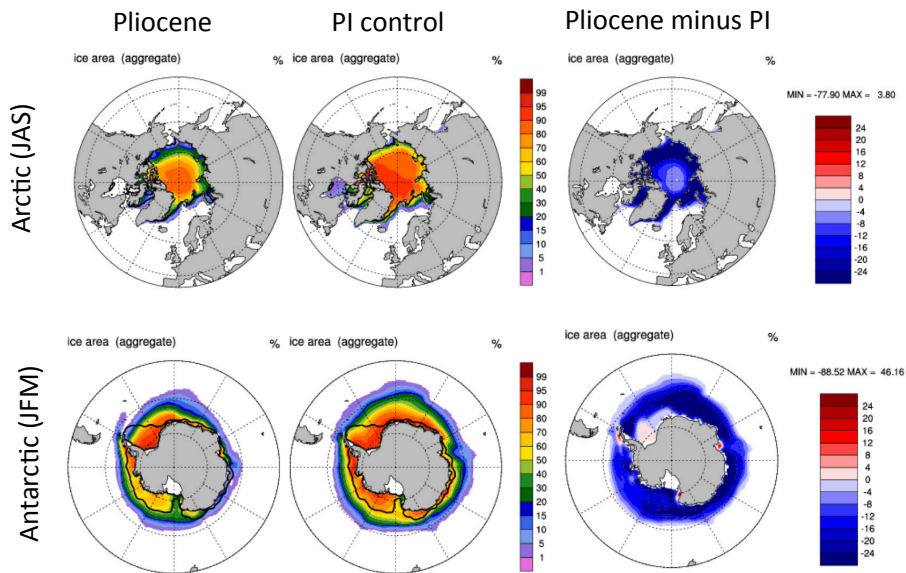
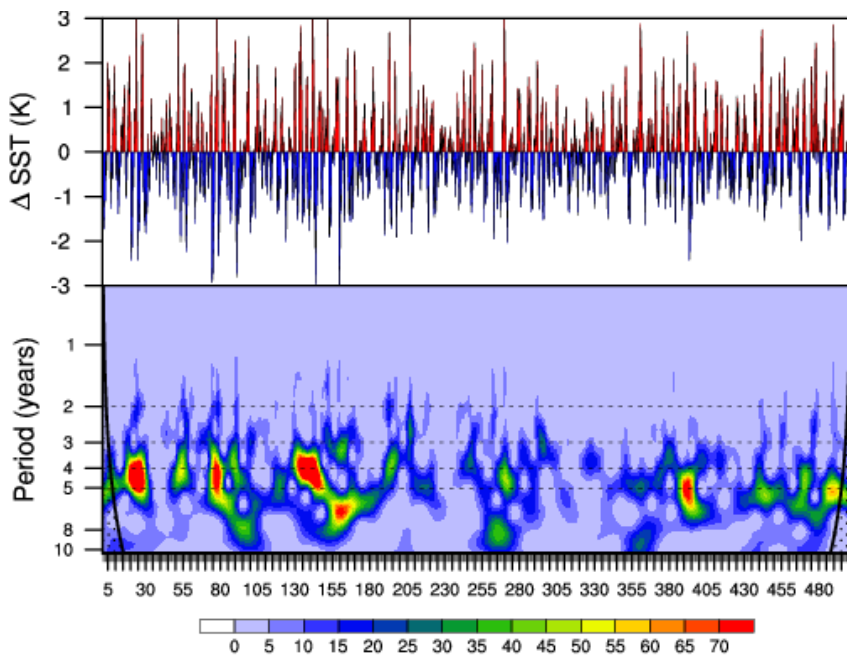


Fig. 8. Spatial maps of Northern Hemisphere (July-August-September) (top) and Southern Hemisphere (January-February-March) (bottom) mean sea ice area [%] for the mPWP, the 1850 PI control, and their difference (mPWP minus PI).

[Title Page](#)
[Abstract](#)
[Introduction](#)
[Conclusions](#)
[References](#)
[Tables](#)
[Figures](#)
[⏪](#)
[⏩](#)
[◀](#)
[▶](#)
[Back](#)
[Close](#)
[Full Screen / Esc](#)
[Printer-friendly Version](#)
[Interactive Discussion](#)

**Simulating the
mid-Pliocene Warm
Period with the
CCSM4 model**

N. A. Rosenbloom et al.

**Fig. 9.** Monthly SST anomalies for Nino3.4.[Title Page](#)[Abstract](#)[Introduction](#)[Conclusions](#)[References](#)[Tables](#)[Figures](#)[Back](#)[Close](#)[Full Screen / Esc](#)[Printer-friendly Version](#)[Interactive Discussion](#)

Simulating the mid-Pliocene Warm Period with the CCSM4 model

N. A. Rosenbloom et al.

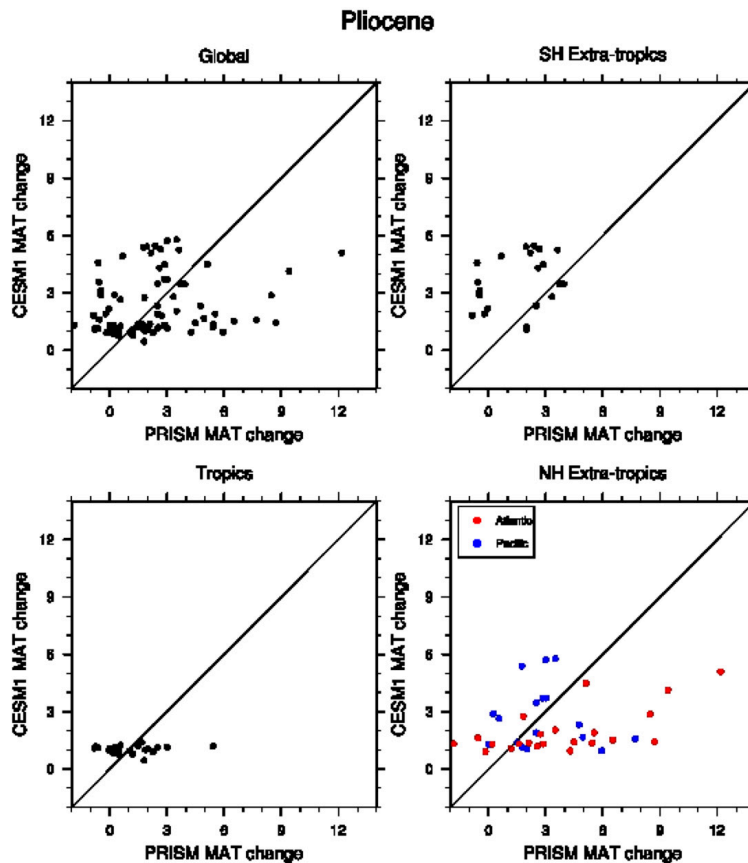


Fig. 10. Regional PRISM3 proxy annual temperature estimates plotted against CCSM4 mean annual temperature for the same latitude/longitude coordinates.

[Title Page](#)[Abstract](#)[Introduction](#)[Conclusions](#)[References](#)[Tables](#)[Figures](#)[⏪](#)[⏩](#)[◀](#)[▶](#)[Back](#)[Close](#)[Full Screen / Esc](#)[Printer-friendly Version](#)[Interactive Discussion](#)

Simulating the mid-Pliocene Warm Period with the CCSM4 model

N. A. Rosenbloom et al.

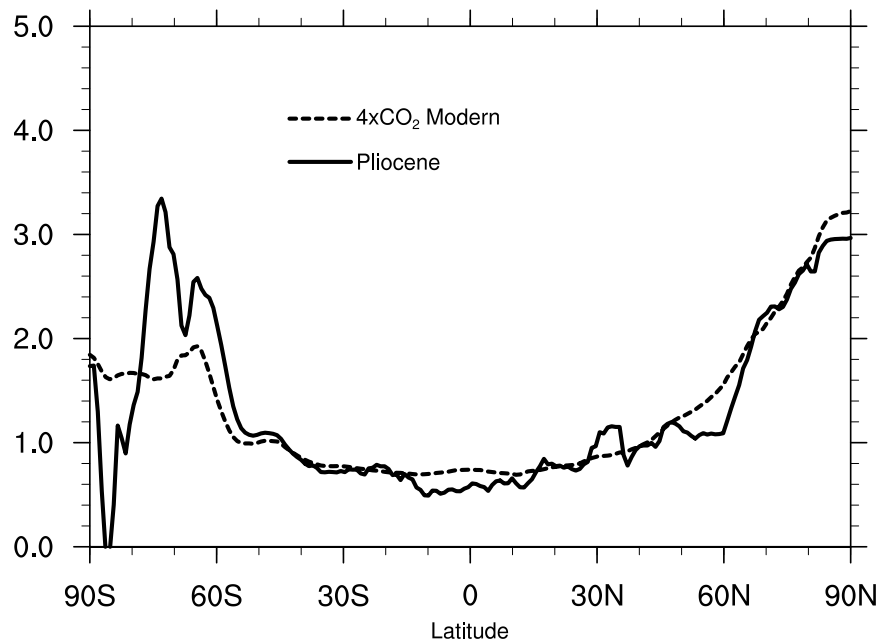


Fig. 11. Zonally averaged MAT anomaly normalized by the global MAT anomaly for the Pliocene (solid line) and abrupt $4 \times \text{CO}_2$ scenario (dashed line).

[Title Page](#)[Abstract](#)[Introduction](#)[Conclusions](#)[References](#)[Tables](#)[Figures](#)[⏪](#)[⏩](#)[◀](#)[▶](#)[Back](#)[Close](#)[Full Screen / Esc](#)[Printer-friendly Version](#)[Interactive Discussion](#)

Simulating the mid-Pliocene Warm Period with the CCSM4 model

N. A. Rosenbloom et al.

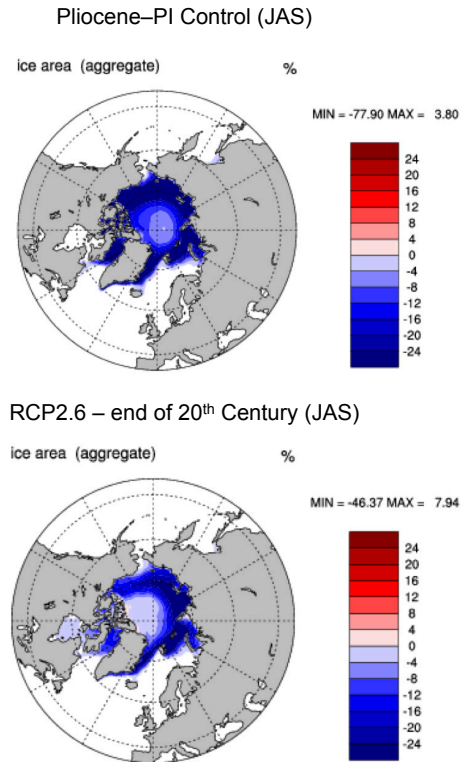


Fig. 12. Spatial maps of the change in NH annual sea ice area [%] in the Pliocene simulation (mPWP minus PI control) (top). Change in NH annual sea ice area [%] in the IPCC RCP2.6 scenario (RCP2.6 (years 2080–2099) minus 20th century (years 1980–1999)) (bottom).

[Title Page](#)
[Abstract](#)
[Introduction](#)
[Conclusions](#)
[References](#)
[Tables](#)
[Figures](#)
[⏪](#)
[⏩](#)
[◀](#)
[▶](#)
[Back](#)
[Close](#)
[Full Screen / Esc](#)
[Printer-friendly Version](#)
[Interactive Discussion](#)